ELSEVIER

Journal of Hazardous Materials A105 (2003) 1–25

Journal of Hazardous Materials

www.elsevier.com/locate/jhazmat

Source, dispersion and combustion modelling of an accidental release of hydrogen in an urban environment

A.G. Venetsanos [a,*], T. Huld [b], P. Adams [c], J.G. Bartzis [a,d]

[a] *National Centre for Scientific Research Demokritos, Environmental Research Laboratory, Institute of Nuclear Technology and Radiation Protection, 15310, Aghia Paraskevi, Attiki, Greece*

[b] *Joint Research Centre of the European Commission, T.P. 450, I-21023 Ispra, Italy*

[c] *Volvo Technology Corp., Dept. 06120 Chalmers Teknikpark, 412 88 Gothenberg, Sweden*

[d] *Department of Energy and Resources Management Engineering, Aristotle University of Thessaloniki, Kozani, Greece*

Received 10 July 2002; received in revised form 5 May 2003; accepted 22 May 2003

Abstract

Hydrogen is likely to be the most important future energy carrier, for many stationary and mobile applications, with the potential to make significant reductions in greenhouse gas emissions especially if renewable primary energy sources are used to produce the hydrogen. A safe transition to the use of hydrogen by members of the general public requires that the safety issues associated with hydrogen applications have to be investigated and fully understood. In order to assess the risks associated with hydrogen applications, its behaviour in realistic accident scenarios has to be predicted, allowing mitigating measures to be developed where necessary. A key factor in this process is predicting the release, dispersion and combustion of hydrogen in appropriate scenarios.

This paper illustrates an application of CFD methods to the simulation of an actual hydrogen explosion. The explosion occurred on 3 March 1983 in a built up area of central Stockholm, Sweden, after the accidental release of approximately 13.5 kg of hydrogen from a rack of 18 interconnected 50 l industrial pressure vessels (200 bar working pressure) being transported by a delivery truck.

Modelling of the source term, dispersion and combustion were undertaken separately using three different numerical tools, due to the differences in physics and scales between the different phenomena. Results from the dispersion calculations together with the official accident report were used to identify a possible ignition source and estimate the time at which ignition could have occurred. Ignition was estimated to occur 10 s after the start of the release, coinciding with the time at which the maximum flammable hydrogen mass and cloud volume were found to occur (4.5 kg and 600 m^3, respectively).

* Corresponding author.

E-mail address: venets@ipta.demokritos.gr (A.G. Venetsanos).

0304-3894/$ – see front matter
doi:10.1016/j.jhazmat.2003.05.001

The subsequent simulation of the combustion adopts initial conditions for mean flow and turbulence from the dispersion simulations, and calculates the development of a fireball. This provides physical values, e.g. maximum overpressure and far-field overpressure that may be used as a comparison with the known accident details to give an indication of the validity of the models.

The simulation results are consistent with both the reported near-field damage to buildings and persons and with the far-field damage to windows.

The work was undertaken as part of the European Integrated Hydrogen Project—Phase 2 (EIHP2) with partial funding from the European Commission via the Fifth Framework Programme.

Keywords: Combustion; Compressed gas; Dispersion; EIHP; Explosion; Hydrogen; Inner city; Street canyon; Release; Urban environment; Safety

1. Introduction

Hydrogen is likely to be the most important future energy carrier, for many stationary and mobile applications, with the potential to make significant reductions in greenhouse gas emissions and significant improvements in the energy efficiency at a global scale, especially if renewable primary energy sources are used to produce the hydrogen, coupled with fuel cells which use this hydrogen to produce electricity.

Hydrogen is particularly attractive for vehicle applications. As a vehicle fuel, hydrogen can be used with either fuel cells/electric drivetrains or internal combustion engines. At present the most attractive options for the onboard storage of hydrogen are as a compressed gas, a cryogenic liquid or as a hydrocarbon reformed on-board the vehicle to produce a stream of hydrogen.

Significant technical problems are associated with the storage of hydrogen. The storage problems arise because of hydrogen's low density. In cryogenic systems operating close to ambient pressure, hydrogen has to be stored at a temperature of approximately 23 K to maintain it in its liquid phase. Compressed gas systems, operate at ambient temperature with working pressures in the region of 200–350 bar and potentially up to 700 bar. It is well known that hydrogen mixed with air forms a flammable mixture over a wide range of mixture concentrations, the lower flammability limit in air being 4% for burning vertically upwards. Ignition may give rise to slow deflagrations, fast deflagrations or under certain conditions detonations depending on the concentration, the size of the cloud and the geometry involved.

A safe transition to the use of hydrogen by members of the general public requires that the safety issues associated with hydrogen have to be investigated and fully understood. In order to assess the risks associated with hydrogen, its behaviour in realistic accident scenarios has to be predicted, allowing mitigating measures to be developed where necessary. A key factor in this process is realistically predicting the release, dispersion and combustion of hydrogen in appropriate scenarios.

A wide range of models of different complexity exists to predict the dispersion phenomena after accidental releases [1]. Compared to the various simpler approaches, e.g. shallow layer type or box models, the computational fluid dynamics (CFD) modelling approach gives more realistic predictions of dispersion in complex geometries [2]. The CFD approach has also been widely used to predict gas explosion phenomena [3], although simple empirical

models also exist, e.g. TNT equivalency methods [4]. However, objections are met if the TNT equivalency concept is used for vapour cloud explosion hazard assessment [5].

Regarding previous hydrogen safety studies, Wilkening et al. [6] performed a safety analysis of liquid hydrogen (LH_2) and compressed gaseous hydrogen (CGH_2) vehicles in a tunnel, by applying CFD methodology for both dispersion and combustion. Two different CFD codes were used in that analysis, one for the dispersion (ADREA-HF [7]) and the other for the combustion (REACFLOW code [8]), due to the differences in physics and scales between the dispersion and combustion phenomena.

In another safety approach Breitung et al. [9], applied CFD to calculate the temporal and spatial distribution of hydrogen and criteria for flame acceleration and detonation potential to estimate the resulting combustion hazard, due to the boil-off from the cryogenic hydrogen tank of a car in a private garage.

In the present paper insight is gained into the modelling of accidental hydrogen releases in built-up, inner city environments referred to as street canyons, which are typical of many European cities. The ADREA-HF and REACFLOW CFD codes are used to simulate a hydrogen accident that occurred in Stockholm in 1983 (official accident report [10]).

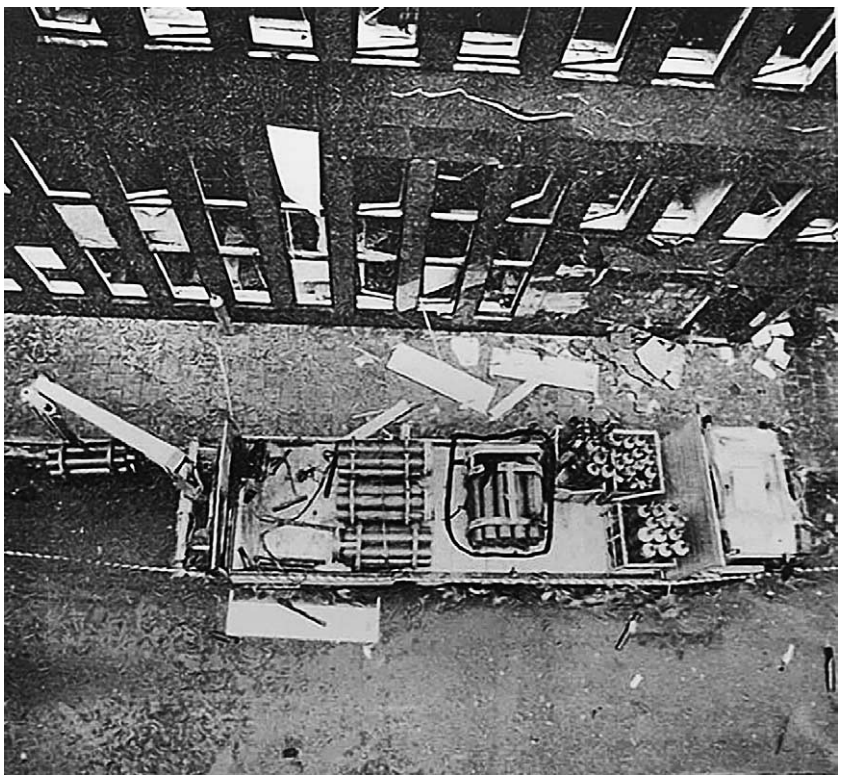

Fig. 1. Truck after the accident. The rack of hydrogen cylinders is marked (picture taken from accident report, with permission).

2. The 1983 Stockholm hydrogen accident

A hydrogen gas explosion occurred just before 9:00 a.m. on Thursday, 3 March 1983 in Brahegatan, a street located in the Östermalm district of central Stockholm, Sweden [10]. An open backed truck was delivering various industrial gases to sites in the Stockholm area. At the site of the explosion a rack of argon gas bottles was being delivered to a laboratory in the building adjacent to the truck (see Fig. 1). The small lifting arm at the back of the truck was being used to offload the argon gas bottles when the operator (truck driver) heard a hissing sound. The operator stopped what he was doing and went to investigate the source of the sound at which point an explosion took place. Approximately 180 N m^3 of hydrogen was stored in a rack of 18 interconnected 50 l industrial pressure vessels (200 bar working pressure) being carried on the back of the delivery truck (Figs. 1 and 2). The official accident investigation found that the release was the result of two broken connections between pressure vessels adjacent to 6 mm diameter T-connection outlets from the cylinders. Shut-off valves were not used to secure the individual cylinders in the rack. The official report stated that one connection was broken, though photographs in the same report clearly show two broken connections (resulting in four release sources).

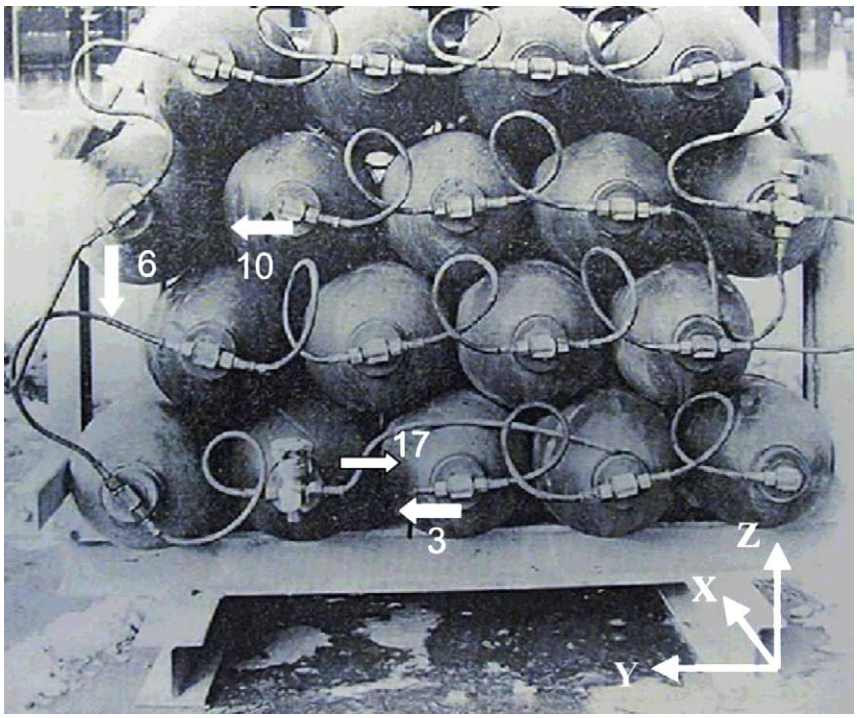

Fig. 2. Hydrogen source, after the accident, comprised of 18 interconnected 50 l steel bottles at 200 bar storage pressure (picture taken from accident report, with permission). The assumed jet directions of the four jets resulting from the two line breaks in the present simulation are shown with arrows. Three of the jets are parallel to the *Y*-axis and one to the *Z*-axis.

The buildings in the area of the accident are primarily residential, typical of inner city Stockholm, with approximately 5–6 floors. The closest building to the explosion was an office block of similar height to the neighbouring buildings. The cross-sectional dimensions of Brahegatan are approximately 2.0 m wide pavements on either side of a 10 m wide carriageway. Parking was permitted on both sides of the street.

The official accident investigation listed the following consequences resulting from the accident:

16 people injured;
10 vehicles damaged;
facade of the nearest building (office block housing a laboratory) was heavily damaged;
broken windows within a radius of approximately 90 m.

A simple analysis of the accident contained in the official accident report estimates that an overpressure of 5 kPa (50 mbar) was experienced at a distance of 90 m from the centre of the explosion, from the damage caused by the explosion. The report estimated that such a shock wave would require 18 N m^3 (1.5 kg) of hydrogen in a deflagration causing a free spherical shockwave and that 10% of the flammable mixture was burned in the explosion, which is consistent with a release of 180 N m^3. The method used to derive this estimation is not stated, though it is likely to be a simple TNT equivalence type method.

3. Mathematical formulation

3.1. Source term

The complicated source system shown in Fig. 2, which is comprised of 18 interconnected tanks, was modelled, by assuming *Fanno* flow in the pipes and isentropic change in the tanks, using real hydrogen properties [11]. The relevant model equations are given below (see [12,13]).

- Pipe mass, energy and momentum conservation:

$$\mathrm{d}(\rho u) = 0, \qquad \mathrm{d}h + u\,\mathrm{d}u = 0, \qquad \rho u\,\mathrm{d}u + \mathrm{d}P + \frac{\lambda}{2}\rho u^2\frac{\mathrm{d}x}{D} = 0 \tag{1}$$

- Tank j mass and energy conservation:

$$\frac{\mathrm{d}V_j\rho_j}{\mathrm{d}t} = \sum_i F_{ij}, \quad i = 0, N_{pj}, \qquad \gamma\frac{\mathrm{d}\rho_j}{\rho_j} = \kappa\,\mathrm{d}P_j \tag{2}$$

where N_{pj} is the number of pipes connected to the tank j and F_{ij} the mass flow rate in pipe i, connected to tank j, positive if the flow is into the tank, V_j the tank j volume, u the pipe velocity, D the pipe diameter, x the distance from pipe entrance, t the time, P the pressure, λ the resistance coefficient (smooth pipes were assumed), $\gamma = c_P/c_V = 1.4$. In the above equations enthalpy h and density ρ were obtained from the following non-ideal gas relations:

- Enthalpy as function of temperature and pressure:

$$\mathrm{d}h = c_P\,\mathrm{d}T + (1-\beta T)\frac{\mathrm{d}P}{\rho} \tag{3}$$

- Compressibility coefficients:

$$\beta = \frac{1}{T} + \frac{1}{z}\left(\frac{\partial z}{\partial T}\right)_P, \qquad \kappa = \frac{1}{P} - \frac{1}{z}\left(\frac{\partial z}{\partial P}\right)_T \tag{4}$$

- Equation of state:

$$z = z(T, P) \equiv \frac{P}{\rho RT} \tag{5}$$

3.2. Dispersion and combustion

The present formulation uses the CFD approach for both the dispersion and combustion calculations. The dispersion and combustion models solve the conservation equations for mass, chemical species, momentum and energy. This set of conservation equations can be written in general integral form [14]:

$$\frac{\partial}{\partial t}\left(\int_\Omega U\,\mathrm{d}V\right) + \int_{S\Omega} n_i F_{i,\mathrm{conv}}\,\mathrm{d}A = \int_{S\Omega} n_i F_{i,\mathrm{diff}}\,\mathrm{d}A + \int_\Omega S\,\mathrm{d}V \tag{6}$$

where $U = (\rho_\gamma, \rho u_j, \rho E, \rho h)^T$ is the vector of conserved quantities which are the unknowns of the system. Here, ρ_γ ($\gamma = 1, \Gamma$) are the partial densities, ρu_j the momentum vector, ρE the total energy (used only in REACFLOW) and ρh the enthalpy (used only in ADREA-HF). The other terms are given as follows:

Convective fluxes:

$$F_{i,\mathrm{conv}} = (\rho_\gamma u_i, \rho u_i u_j + p\delta_{ij}, \rho u_i(h + \tfrac{1}{2}u_i^2), \rho u_i h)^T \tag{7}$$

Diffusive fluxes:

$$F_{i,\mathrm{diff}} = \left(D_\gamma \frac{\partial Y_\gamma}{\partial x_i}, \tau_{ij}, \sum_{\gamma=1}^{\Gamma} h_\gamma D_\gamma \frac{\partial Y_\gamma}{\partial x_i} + \lambda\frac{\partial T}{\partial x_i} + \tau_{ij}u_j, \sum_{\gamma=1}^{\Gamma} h_\gamma D_\gamma \frac{\partial Y_\gamma}{\partial x_i} + \lambda\frac{\partial T}{\partial x_i}\right)^T \tag{8}$$

Source terms (including chemical reactions, for REACFLOW only):

$$S = \left(-\dot{\rho}_\gamma, -\rho g_j, -\rho g_j u_j - \sum_{\gamma=1}^{\Gamma} \dot{\rho}_\gamma \Delta h_\gamma^{\mathrm{f}}, \frac{Dp}{Dt}\right)^T \tag{9}$$

where h_γ, Y_γ ($\gamma = 1, \Gamma$) are the partial enthalpies and mass fractions, $\dot{\rho}_\gamma$, the chemical production rates, $\Delta h_\gamma^{\mathrm{f}}$ the formation enthalpies, g_j the acceleration of gravity, T the temperature, τ_{ij} the shear stress tensor, D_γ the scalar transport diffusivities and λ the effective conductivity.

Closure of this system of equations is done with an equation of state, which for both the dispersion and the combustion codes is a variant on the equation for an ideal mixture of gases. Real hydrogen compressibility factors [11] were used in the dispersion code. Temperature dependent mixture components heat capacities [11] were used in both codes.

In both codes turbulence is modelled using the eddy viscosity formulation.

In the dispersion code it is simulated using a non-isotropic one-equation turbulence model, which solves the turbulent kinetic energy and employs analytic formulas to derive the length scales, which depend on distance from the nearest solid, stability and global acceleration parameter (see [15]).

The combustion model employs a compressible version of the classical two-equation $k-\varepsilon$ equations. The turbulent quantities serve to calculate the turbulent viscosity for the Favre-averaged flow equations. At the same time the turbulent quantities are employed as input for a model for the turbulent combustion. The model employed is a modified version of the Eddy-dissipation model proposed by Hjertager [16]. In this model, the source term for the fuel is given by

$$\dot{\rho}_{\mathrm{f}} u = -c_{\mathrm{f}} \frac{4.4}{1 + 3.2\sqrt{k}/S_{\mathrm{L}}} \rho Y_{\mathrm{lim}} \frac{\varepsilon}{k} \tag{10}$$

where k is the specific turbulent kinetic energy, ε the specific turbulent kinetic energy dissipation rate, S_{L} the laminar burning velocity, and Y_{lim} the mass fraction of the "limiting" chemical species, i.e. the reacting chemical species present in the lowest concentration (weighted by the stoichiometry of the species in the reaction) at a given time during the combustion process.

For hydrogen combustion in dry air, when a given volume of mixture begins to burn, Y_{lim} will at first be equal to the mass fraction of water and the value will be very low. As the burning proceeds the water concentration rises and with it the reaction rate. When the (stoichiometrically weighted) water concentration exceeds that of hydrogen or oxygen the limiting species will become hydrogen (for lean mixtures) or oxygen (for rich mixtures), and the reaction rate will decrease. Note that this should not be thought of as an accurate description of the chemical kinetics. Rather, it is a model of the way the turbulent flame propagates through a small but finite volume. When the flame just enters a given volume the average reaction in the volume will be low because of the small flame area. As the flame expands in the volume the average reaction rate increases and then decreases again as the flame front leaves the volume.

The laminar flame speed S_{L} depends on the local hydrogen concentration. In the calculations it has been assumed to vary in a polynomial fashion, with a polynomial fitted from published data [17].

c_{f} is basically an empirical factor. For the present calculations we have used the published values by Hjertager [18].

The limitations of this model lie in the extremes of a turbulent deflagration event, where the turbulence is very weak the k and ε values become very small, and the ratio ε/k becomes very uncertain. At the other extreme, this model does not handle a transition to detonation very well since the physics of a detonation is very different from that of a turbulent deflagration. In the model the combustion rate does not depend directly on temperature or pressure but is governed by the rate of turbulent mixing. It therefore cannot adequately handle detonation

processes where the combustion is driven by adiabatic compression by the shockwave heating the unburned mixture to above the ignition temperature.

4. Modelling strategy

4.1. Source

The official accident report shows that two breaks occurred in the lines connecting the pressure vessels, one near the left side of the bundle and the other near the bottom (see Fig. 2). It can also be seen that the bottom break is fed by a system of three interconnected cylinders, which is entirely disconnected from the remaining 15 interconnected cylinders.

In order to estimate the released hydrogen mass at the time of the explosion, it is important to know whether the two breaks existed before the explosion or one of them was the result of the explosion. To investigate on this effect release calculations were performed for one and two line breaks (two and four jets, respectively). The diameter of the line connecting the cylindrical vessels was assumed of 6 mm and its length of 300 mm. No losses were taken into account due to the T-connection outlets from the cylinders. Calculated hydrogen release mass–time histories are shown in Fig. 3 for the following cases:

Case 1: the first curve corresponds to the detailed modelling of all 18 vessels, assuming 4 jets, as shown in Fig. 4. The sudden drop at approximately 50 s is because of the emptying of the three vessels that feed jet 3.

Case 2: the second curve corresponds to the detailed modelling of all 18 vessels, assuming 2 jets (nos. 3, 17). The sudden drop at approximately 50 s is because the three vessels that feed jet 3 are empty.

Case 3: the third curve corresponds to the detailed modelling of all 18 vessels, assuming 2 jets (nos. 6, 10). There is no sudden drop in this case, because there is no independent system of vessels as was in Case 2.

Comparing Cases 1–3 it can be observed that the time period needed for the entire system to be empty is much less in Case 1 than in Cases 2 and 3. For Case 1 this period is approximately 75 s, which is approximately in agreement to the 60 s estimated in the accident report, although it is not stated there whether this estimation was the result of one or two breaks. Due to this agreement the results of case 1 were supplied as input to the ADREA-HF dispersion calculations.

Regarding the time of the explosion, we have assumed 10 s after start of release, on grounds explained in the results section below. It can be observed from Fig. 3 that even at this early time the difference between Cases 1–3 is important. It can also be observed that as the explosion time goes to zero (explosion very close to start of release) the difference between Cases 1–3 becomes less important.

Fig. 3 also shows predicted hydrogen mass–time histories for the following cases:

Case 4: the fourth curve represents a simplified system comprising one vessel with a volume of 900 l (18 × 50 l) and a single jet from a pipe 300 mm in length and 6 mm in diameter.

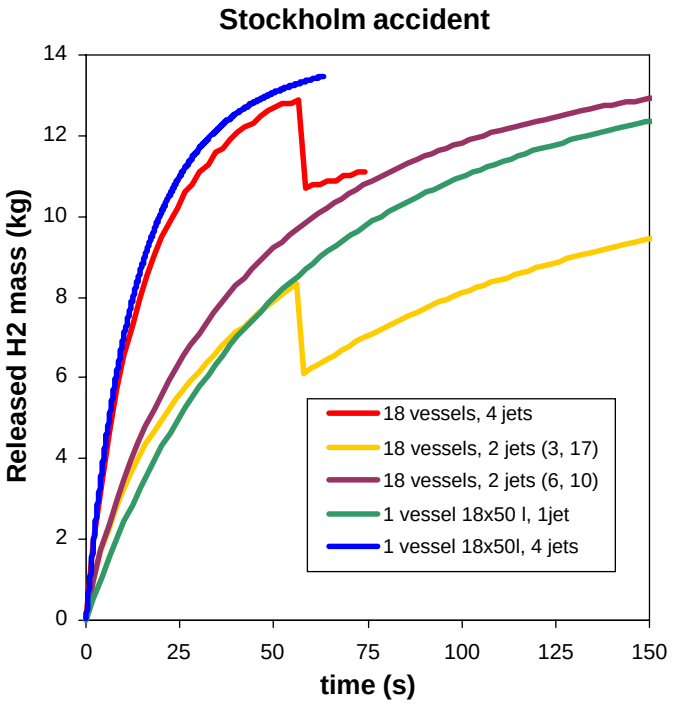

Fig. 3. Predicted released hydrogen mass as a function of time (see Fig. 2 for jets numbering).

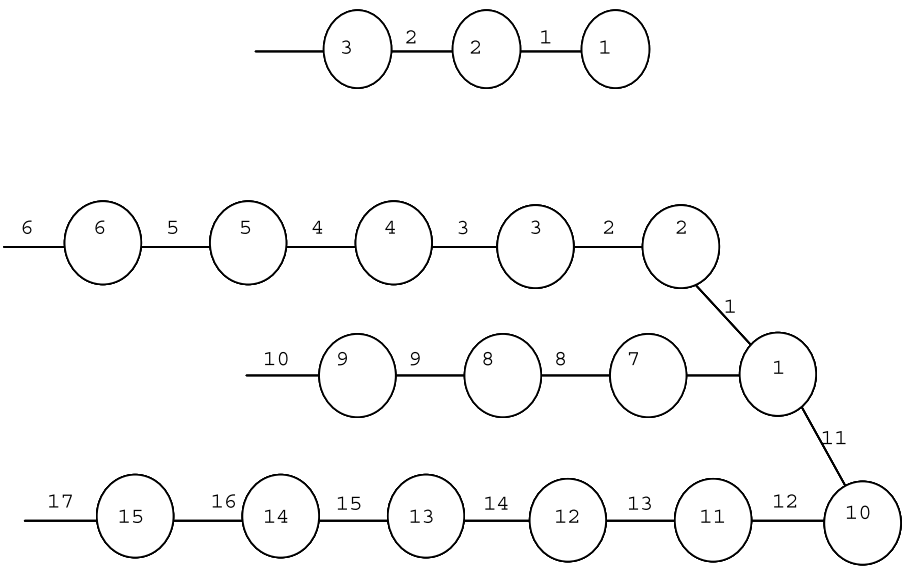

Fig. 4. Stockholm accident source modelled as two separate sources, comprised of 15 and 3 cylinders, respectively.

Case 5: the fifth curve shows the total released mass obtained using a single vessel with a volume of 900 l as in Case 4, but with four jets instead of one.

Comparing Case 5 to Case 1 it can be observed that in Case 5 the released mass is overestimated only by 4% with respect to the more complex Case 1, at 50 s after the start of release.

4.2. Dispersion

The boundary of the modelled area of the city is shown in Fig. 5 (dotted line). The domain dimensions were 380 m × 440 m × 180 m in the *X*-, *Y*- and *Z*-directions, respectively. The plan view of the grid and buildings is shown in Fig. 6. The buildings were assumed to be six stories high with inclined 45° roofs and internal courtyards. From aerial photos it was estimated that the buildings are approximately 14 m wide. The grid was Cartesian

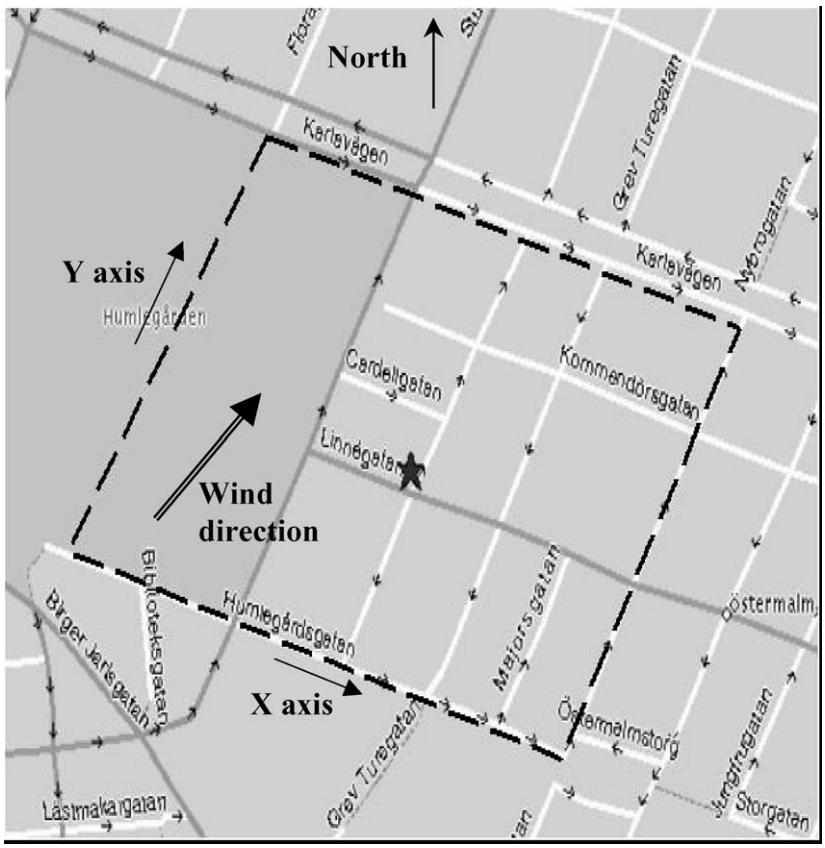

Fig. 5. Horizontal domain of the dispersion model marked by dotted line on the Stockholm city map (map from http://www.mapquest.com). Angle between the *X*-axis of the domain and the north direction is 110°. Angle between the ambient wind direction and the *X*-axis is 70°.

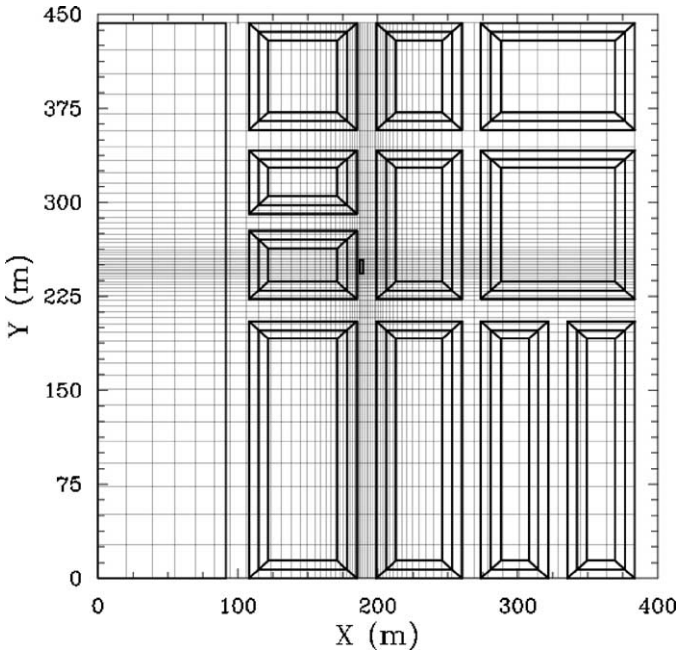

Fig. 6. Horizontal grid used in the dispersion calculations. Shown are the modelled buildings and truck footprints.

non-equidistant comprised of 60 × 58 × 41 cells. The minimum horizontal cell dimension was 1.4 m close to the source. The minimum vertical cell dimension was 0.5 m close to ground. The grid expansion ratio was 1.12. The truck was assumed to have length of 11 m, width of 2.5 m and platform height of 1.25 m.

As can be observed in Fig. 6 the solids (buildings and truck) were placed in the grid by permitting their boundary surfaces to cross the computational cells. The ADREA_HF code is able to account for partially blocked cells using the porosity formulation. The cell volume and area porosities were calculated using the geometrical pre-processor DELTA_B [19].

The four jets comprising the source were assumed to have directions as shown in Fig. 2.

The meteorological conditions for the Stockholm area on the day and time of the accident were obtained from the Swedish Meteorological and Hydrological Institute (SMHI). The observations at Bromma airport on 3 March 1983 at 9:00 a.m. local time were: wind speed 2 knots (1.03 m/s), meteorological wind direction 220° (corresponds to 70° from X-axis—see Fig. 5), air temperature −4 °C and 98% relative humidity. In the dispersion calculations the atmospheric stability was assumed to be neutral.

The dispersion calculations were performed in three stages. At first the vertical velocity profile that matched the Bromma meteorological observations was calculated (the Bromma data were assumed to correspond to 10 m elevation). The energy equation was not solved. The temperature profile was calculated from the adiabatic lapse rate ($\mathrm{d}T/\mathrm{d}z = -g/c_P$) and the Bromma observation.

In the second stage the steady state wind field over the three-dimensional building geometry was obtained. The energy equation was not solved in this case. Initialisation of the

velocity, turbulent kinetic energy and temperature fields was performed, by spreading the vertical profiles from the first stage over the entire 3D domain. Dirichlet (given value) plus Neumann (zero gradient) boundary conditions were used for the inflow domain lateral planes (west and south in Fig. 6). Neumann boundary conditions were used for the outflow domain lateral planes (east and north in Fig. 6). Wall functions for velocity and turbulent kinetic energy were used at the ground and building walls. Neumann boundary conditions were used at the top of domain, except for the w-velocity, for which a zero value was assumed.

The third stage involved the transient release of hydrogen. This stage initiated from the previously obtained steady state results. The energy (enthalpy) and hydrogen conservation equations were also solved during this stage. Boundary conditions for these equations were Dirichlet plus Neumann at the inflow planes and Neumann at the outflow planes, ground and buildings. Finally, at the jet surfaces Dirichlet plus Neumann boundary conditions were used for all the variables, where jet exit velocities, temperatures and pressures were functions of time, obtained from the previous source model calculation.

4.3. Combustion

The simulations of the combustion event were made as a two-step process. In order to perform an accurate simulation of the initial flame acceleration and the combustion of the central part of the cloud where concentrations were the highest, a simulation with a fine spatial resolution was used for the initial part of the combustion event. Based on the results of this simulation, a second simulation was performed in a larger domain with a coarser grid to estimate the far-field overpressure. The estimate of the far-field overpressure is important for comparing the results of the modelling with the reported accident consequences.

The initial part of the combustion event was simulated using an unstructured tetrahedral grid in a region of dimensions 14 m × 35 m × 18 m, thus spanning the 14 m wide street up to a height of 18 m, i.e. up to the start of the slanting roofs.

Due to the relatively fine grid resolution it was possible to include some extra geometrical details around the truck. In this way the driver cabin is represented, as well as some of the

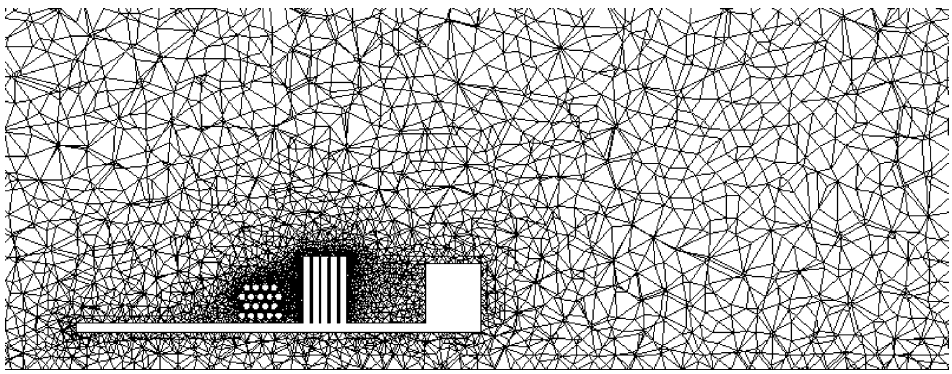

Fig. 7. Vertical cut (at a distance of 2.15 m from the building wall) through the grid for the first part of the combustion simulation. This cut passes through the hydrogen cylinders, which show up in the figure as white circles. Note the varying grid density and the presence of the adjacent vertical pressure vessels.

pressure vessels standing on the back of the truck, some in a horizontal position and some in a vertical position.

The grid density varies, from a minimum distance of $\Delta x \approx 0.08$ m in the vicinity of the hydrogen tanks, to a grid distance of >0.25 m far away from the truck. The total number of grid points in the initial grid, were app. 78,000. Fig. 7 shows a vertical cut through the domain at a position of $x = 2.31$ m, just inside the truck.

Initial conditions were obtained from the dispersion simulations by interpolation onto the computational grid used for the combustion simulations. The values for temperature, pressure, velocities and hydrogen concentration were taken from the dispersion simulations. The rest of the gas cloud mixture was assumed to be dry air.

Possible ignition sources were not stated in the accident report. For the purposes of the simulation the ignition point was assumed to be at the surface of the truck between the vertical pressurised tanks adjacent to the rack of hydrogen vessels (see Fig. 1). While the actual ignition point is not known, this is a plausible site since the vibrating truck may caused sparks

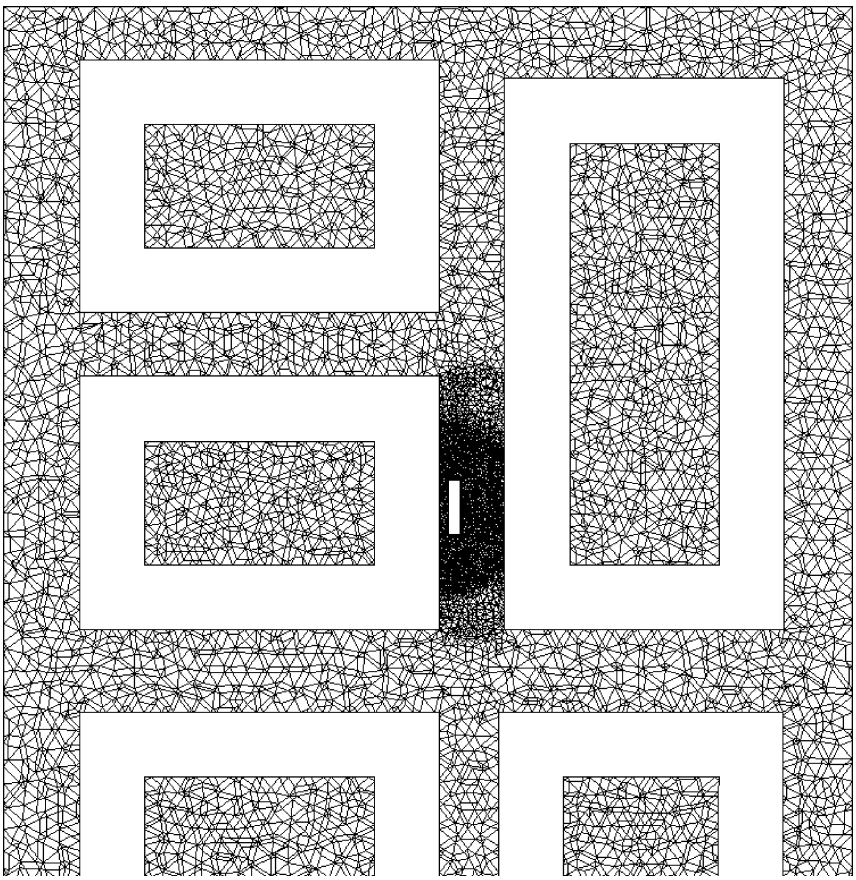

Fig. 8. Horizontal cut (at $z = 1.2$ m) through the grid used for the second stage of the combustion calculation. The rectangular cut-outs represent the houses in the area.

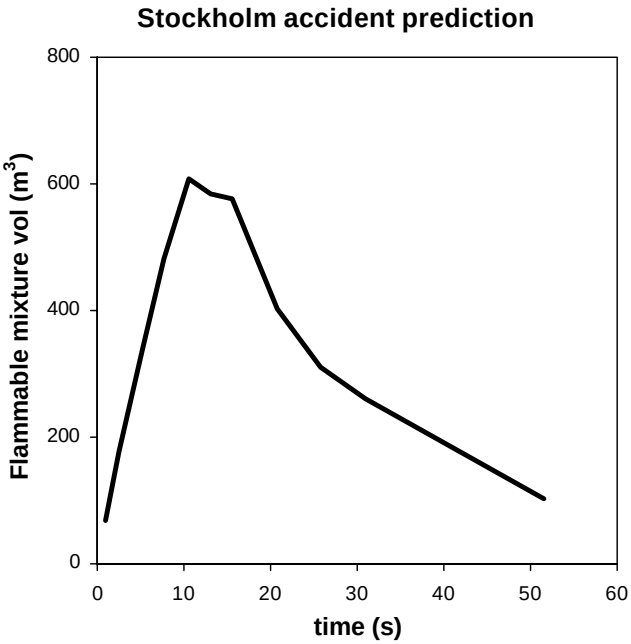

Fig. 9. Predicted time history of the flammable hydrogen–air mixture volume (4–75% hydrogen concentration).

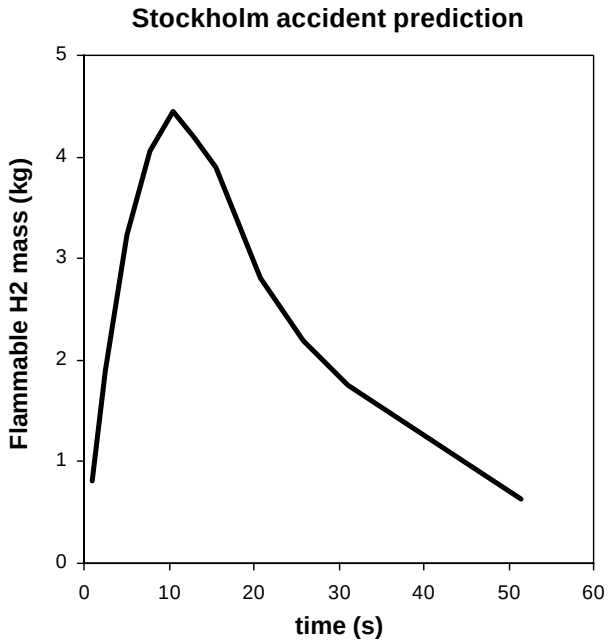

Fig. 10. Predicted time history of the flammable hydrogen mass (4–75% hydrogen concentration).

between the truck surface and the rack of vertical pressure vessels. The ignition was modelled by assuming a small spherical region to be at a high temperature and partially burned.

The simulation employed a dynamically adaptive grid [8]. The adaptation criterion was chosen to be the difference in temperature. Due to this adaptation, the number of grid points rose from the initial 78,000 to a maximum of app. 300,000 as the flame front expanded.

The second stage of the combustion simulation used a grid on a larger spatial domain, of dimensions 182 m × 200 m × 30 m for a total of app. 26,000 nodes. Here the minimum grid distance in the region around the truck was much larger than in the first simulation, with $\Delta x \approx 0.3$ m rising to >3 m at the corners of the domain. The pressure vessels are not resolved in this grid. Fig. 8 shows a horizontal cut through this domain at $z = 1.2$ m. The initial conditions for this calculation were taken from the first combustion simulation at a time $t = 90$ ms using interpolated values from the full adapted grid of the first simulation. For this calculation the grid adaptation was made using pressure differences. The original number of app. 26,000 nodes rose during the calculation to a little over 100,000 nodes before falling back due to the very low pressure differences towards the end of the simulation time of $t = 1$ s.

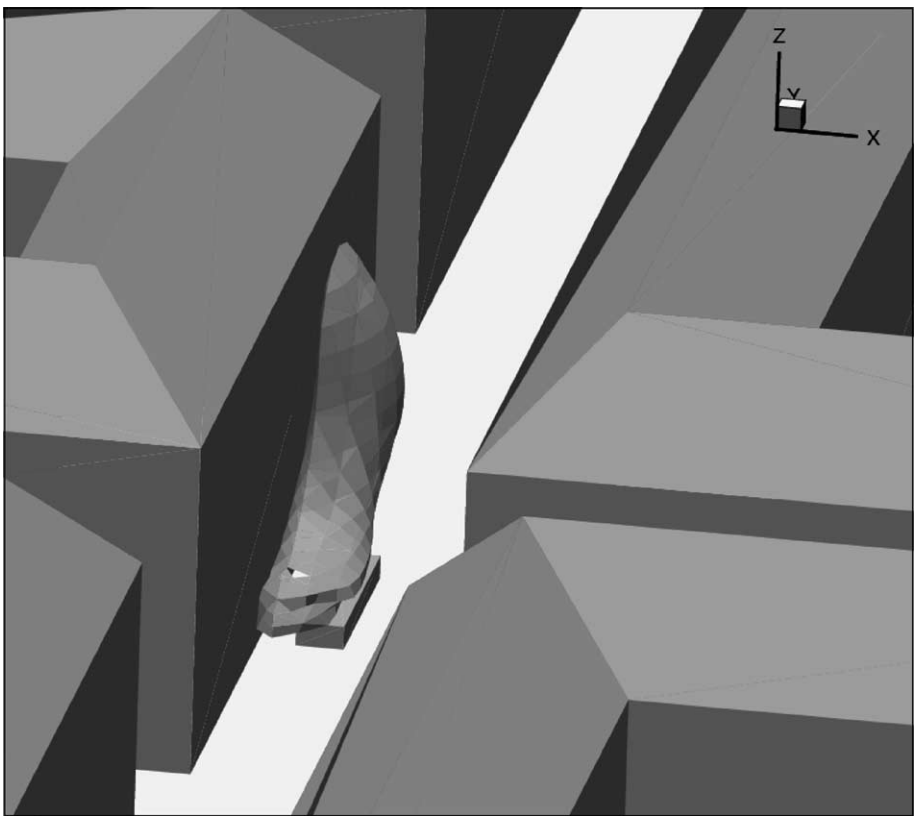

Fig. 11. Predicted flammable cloud (4% hydrogen concentration iso-surface) at time 10 s after start of the release.

5. Results and discussion

Fig. 9 shows the predicted volume of the flammable hydrogen air mixture, i.e. where hydrogen volume concentration is between the lower and upper flammability limits (4 and 75%, respectively). Fig. 10 shows the mass of hydrogen contained in the flammable cloud. It can be observed that at about 10 s after the start of the release, the proportion of hydrogen in a flammable concentration with air peaks (approximately 600 m^3 cloud volume/4.5 kg of released hydrogen in flammable proportions with air). The peak 10 s after the release starts, while the release continues for some 60 s, is due to the turbulent mixing between hydrogen and ambient air. If turbulent mixing did not exist then the peak in the curve of released hydrogen mass versus time would be at the end of the release period (see Fig. 4).

Figs. 9 and 10 were used together with accident reporting to estimate when to start the combustion calculations. Based on the accident report, the driver of the vehicle heard a hissing sound while unloading a bundle of argon gas bottles with a small lifting arm mounted on the rear of the truck. As the driver went to investigate the sound, a powerful explosion occurred in the vicinity of the vehicle. The time period between the start of the release, the driver hearing and reacting to the sound and the explosion was estimated by the authors to be 5–10 s. For the calculations the time of ignition was assumed to be 10 s after the start of the release, coinciding with the time at which the maximum flammable hydrogen mass and cloud volume occurred according to Figs. 9 and 10.

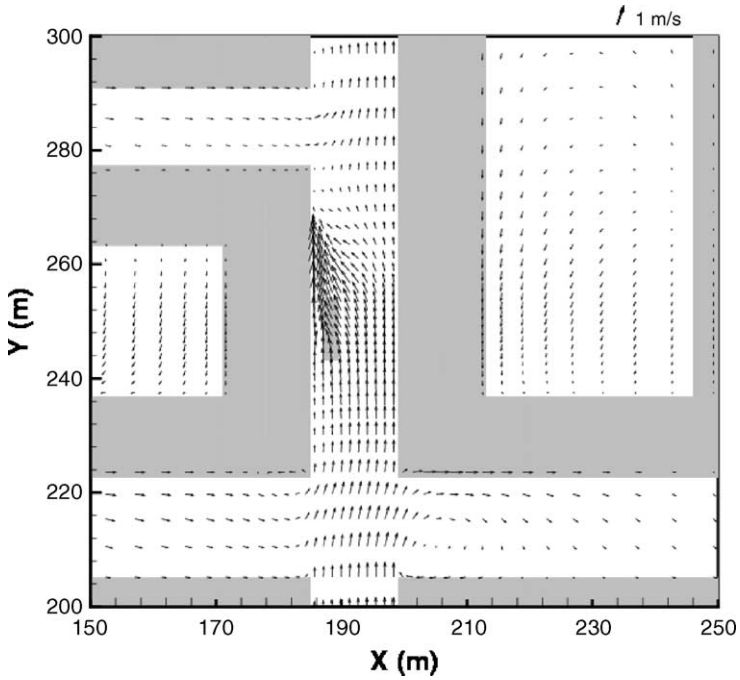

Fig. 12. Predicted horizontal velocity field at 3.4 m from ground and time 10 s after start of the release. The reference vector shows the ambient wind direction (70° from *X*-axis) far above the buildings.

Fig. 11 shows Brahegatan, the truck and the predicted shape and position of the 4% concentration cloud, 10 s after the start of release. It was assumed that the flammable cloud was ignited near its base. The lower flammability limit for upwards burning (4%) was assumed to be valid. The dispersion modelling suggests that the cloud did not spread transversely across the street to a significant degree, only in between the truck and the nearby building. Along the street, the cloud appears to drift away from the truck, increasing in height with increasing distance from the truck. The predicted cloud behaviour is explained below by examining the flow and dispersion patterns at 10 s.

Fig. 12 shows the predicted horizontal velocity field, at a distance of 3.4 m from the ground, in a region of 100 m × 100 m around the truck. In general, as a result of the assumed light wind conditions based on the Bromma observations, low wind velocities were obtained within the street canyons, far from the source (see also Figs. 13–15). In Brahegatan the main flow direction is along the street, obviously due to the assumed external wind direction. Close to the source of the release there are strong horizontal velocities along the street, which show that the local flow is strongly affected by horizontal jet momentum.

The strong horizontal jet momentum effects can also be observed in Figs. 13 and 14. Fig. 13 shows the predicted flow field and dispersion patterns on the horizontal plane at 0.8 m elevation, close to the truck and Fig. 14 on the vertical plane along the street canyon, at $x = 186$ m, i.e. 1 m between building and truck. The previous figures show that jet

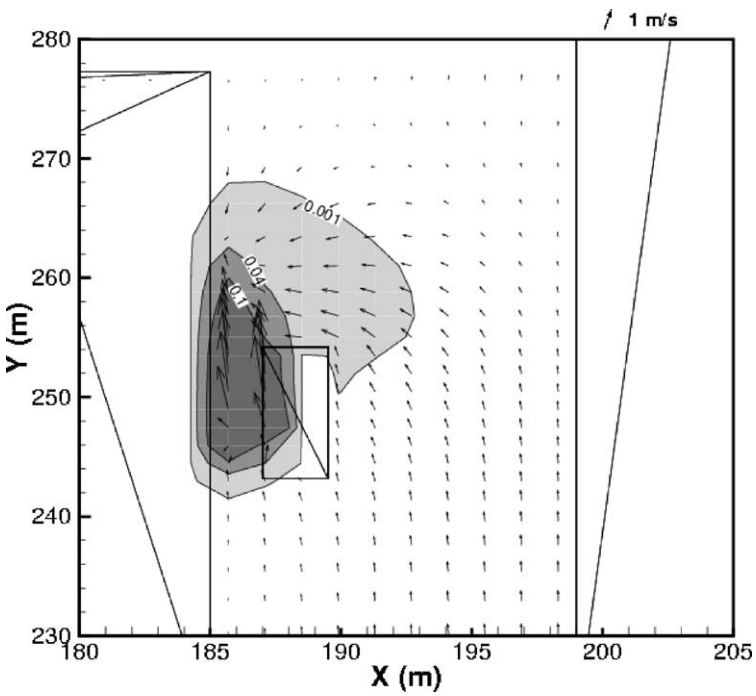

Fig. 13. Predicted horizontal velocity and volume concentration field at 0.8 m elevation and time 10 s after start of the release. The reference vector shows the ambient wind direction far above the buildings.

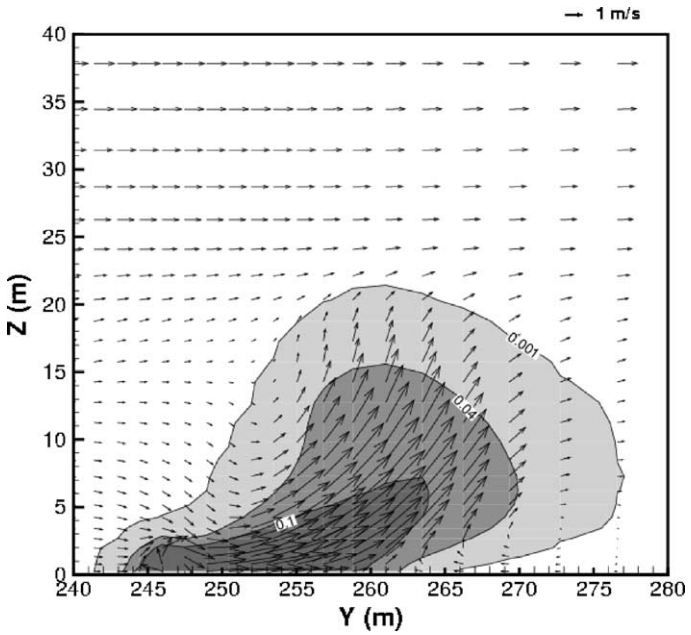

Fig. 14. Predicted velocity and volume concentration field on a vertical plane along the street canyon, midway between the source and the nearby building 10 s after start of the release.

momentum is dominant in the positive *y*-direction and this was expected since two of the four jets at the source were assumed to be pointing in that direction (see Fig. 2). Fig. 14 also shows that close to the source there is a region of downward flow. This is attributed both to the downward momentum of the vertical jet at the source (see Fig. 2) and the negative buoyancy effects at the source. The latter effect is the result of the very low jet exit temperatures. Of the two effects the former is considered to be dominant.

Close to the source the cloud buoyancy is negative, while it is strongly positive further away from it as hydrogen temperatures approach that of the surrounding environment, and because of the very low molecular weight of hydrogen (2) with respect to air (28). This effect is clearly seen in Fig. 14, where strong buoyancy gives rise to vertical flow, which transports the flammable cloud up to 15 m above the ground. This upward motion causes the flow after the truck to turn towards the building as observed in Fig. 13. The same rising flow effect is seen in Fig. 15, which shows the predicted cross-street flow and dispersion patterns at $y = 257$, i.e. approximately 9 m along the street from the source.

Fig. 15 also shows that the strong vertical movement of the cloud on the truck side of the street is mainly responsible for the cross-street flow towards the truck (see also Fig. 11) and not the external cross-street flow, which is very weak obviously because of the assumed external flow direction. This cross-street flow towards the truck due to the wind conditions assumed tends to restrict the cloud from spreading across the street.

The above dispersion results had a direct implication for the subsequent combustion modelling strategy. It had been thought that one of the streetlights that were hung across

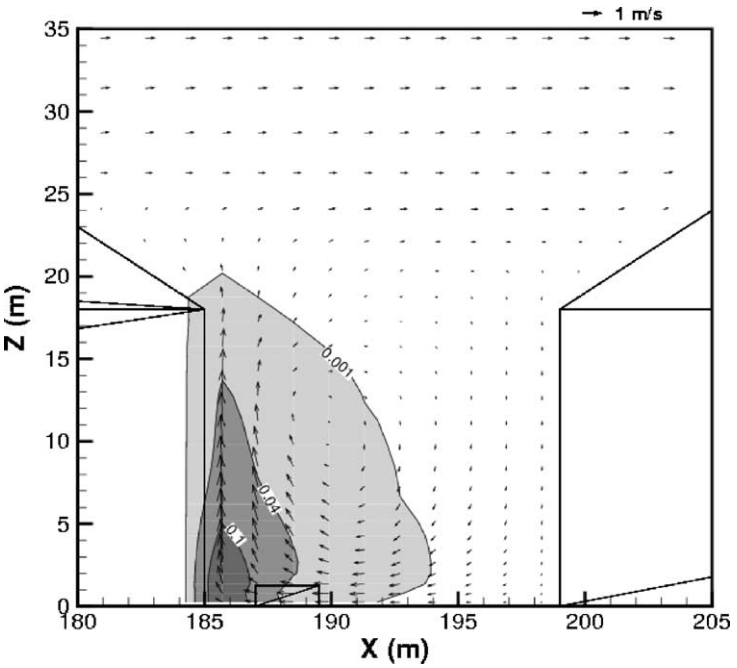

Fig. 15. Predicted velocity and volume concentration field on a vertical cross-canyon plane at 9 m downwind from the source and time 10 s after start of the release.

the street, at a height of approximately 8 m, could have been the ignition source. Fig. 11 suggested that this was unlikely and that the ignition source had to be somewhere in the vicinity of the truck and the nearby building. It was assumed to be at the surface of the truck between the vertical pressurised tanks adjacent to the rack of hydrogen vessels (see Fig. 1).

The accident report indicated that windows were broken at a distance of up to approximately 90 m from the explosion. It can be assumed that the 90 m radius represents the threshold of window breakage. Additionally the accident report suggested that an overpressure of 5 kPa (50 mbar) was required to break windows though no references were given. The estimated peak overpressure of 50 mbar at 90 m is considered to be a significant overestimate. Most sources of explosion damage data indicate that the threshold of window breakage (10% broken windows) occurs at approximately 20 mbar. For this work 25 mbar was taken as the threshold of window damage as most windows in residential buildings in Sweden are double glazed, if not triple glazed, with an inherently higher blast resistance.

The combustion simulation shows that an initially slow (laminar) flame accelerates due to the turbulence generated by the geometrical obstacles in the vicinity (primarily the pressure tanks). Since the hydrogen cloud is very concentrated, with a large region with more than 15% hydrogen by volume, there is ample scope for flame acceleration. However, the general geometrical configuration is rather open, and beyond the bundles of pressure tanks there are few obstacles. This will tend to restrain the acceleration of the flame and prevent the flame from accelerating to very high speeds as seen in the simulations.

Fig. 16. 2D plane cut for a vertical plane at $x = 2.31$ m (distance from the building wall) showing the hydrogen volume concentration at $t = 0$ ms (corresponding to $t = 10$ s in the dispersion simulation). Colours indicate a range of concentrations from 0.04 (dark blue) to 0.3 (very light blue). Black regions indicate a concentration of less than 0.04 (not flammable).

Fig. 16 shows the hydrogen concentration (percentage by volume) in a plane through the truck near the side of the truck closest to the pavement (at $x = 2.31$ m). The concentration reaches nearly 30% in a fairly large volume but decreases rapidly with distance from the source. The highest concentrations are found in regions with few turbulence-inducing obstacles.

Fig. 17 shows the evolution of the initial flame from the ignition near the lower end of the vertical cylinders. At first the flame expands slowly but then it accelerates and in less than 70 ms it has grown from a fairly small fireball to one engulfing the entire truck. The flame speed varies strongly with position but in some points it exceeds 100 m/s. However, there is no indication that the flame speed approaches sonic speed anywhere in the fireball. This corresponds to a combustion regime, which is clearly turbulent but not the equivalent of a fast deflagration.

The pressure is shown in Fig. 18 as a function of time for a single point near the building wall. The maximum overpressure is a little over 100 kPa (1000 mbar). The position of the measuring point near the wall, where the pressure wave is reflected from the wall, means that this pressure is higher than the pressure further away from the wall. The maximum overpressure is consistent with the estimate of the flame velocity showing a “slow turbulent flame”. The pressure figure is also consistent with the reported accident damage which showed some damage to the building walls but not a complete collapse of the building

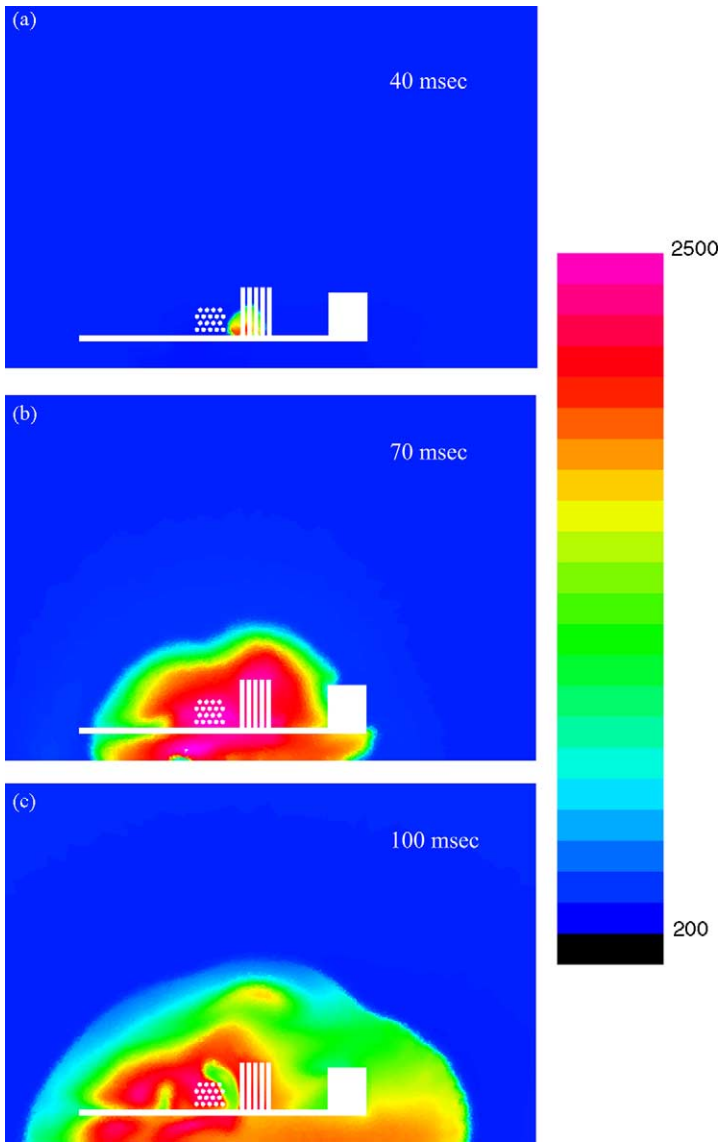

Fig. 17. 2D plane isothermal plots for a vertical plane at $x = 2.31$ m (distance from the building wall) in a region around the truck. Fields shown are temperature at three different times: (a) $t = 40$ ms; (b) 70 ms; (c) 100 ms. Colours represent temperatures in the range of 200–2500 K.

façade as might have happened if the maximum overpressure had been considerably higher. The fact that no fatalities were noted in the official accident report suggests that any people near the explosion survived and that the pressures did not rise above the maximums obtained in this simulation.

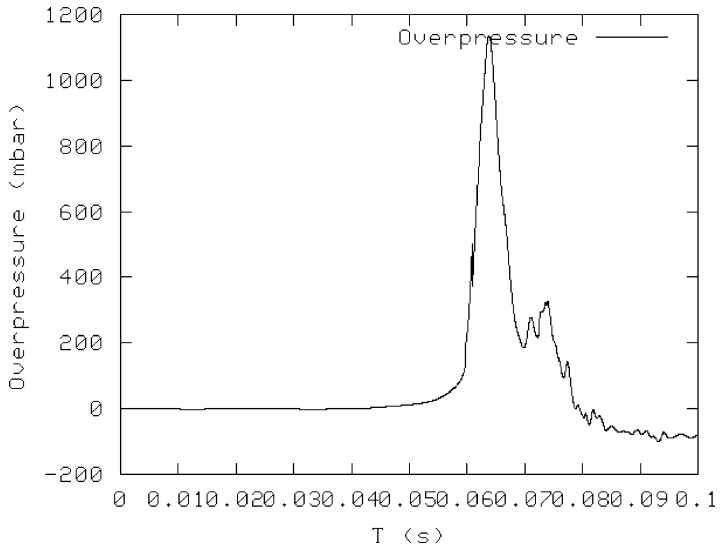

Fig. 18. Plot of overpressure with time for a single point. This point is placed at $(x, y, z) = (0.05, 6.0, 1.35)$, which corresponds to a point near the building wall at a height of 1.35 m and a position along the street (y-direction) close to the rear end of the truck.

One of the relatively few pieces of information from the accident report, which may be used to make a direct comparison with the simulated results, is the distance at which the pressure wave from the explosion caused windows to break. To simulate this it was necessary to perform a simulation in a domain much larger than the one used to simulate the initial evolution of the flame. The computational grid used for this simulation is described in Section 4.

Figs. 19 and 20 show overpressure values as functions of time for five different locations along the street where the explosion occurred. Fig. 19 shows the overpressure at three different positions along the street in front of the truck, at distances approximately 3.5, 13 and 23 m from the ignition point, in a position close to the wall and at a height of 1.35 m above the pavement. It is clearly seen that the maximum overpressure decreases with increasing distance from the truck. It is also clear that the overpressure is sufficient to cause windows to break. It should be noted that in the present calculations, the flammable hydrogen mass at the start of the explosion, which burned later was 4.5 kg (Fig. 10), which is much higher than the accident report estimate of 1.5 kg (18 N m^3) burned in the explosion, while in both works overpressures consistent with reported damage are implied. This consistency in case of the accident report is because TNT equivalence methods (which were probably used) overestimate the overpressures close to the centre of the explosion [4].

Fig. 20 shows the overpressure at two locations further down the street, at approximately 27 and 45 m from the ignition point. Overpressures are considerably lower here, and at the street corner (45 m from ignition) they are so low that windows in this position might not break. According to the accident report windows did in fact break also at this distance. The

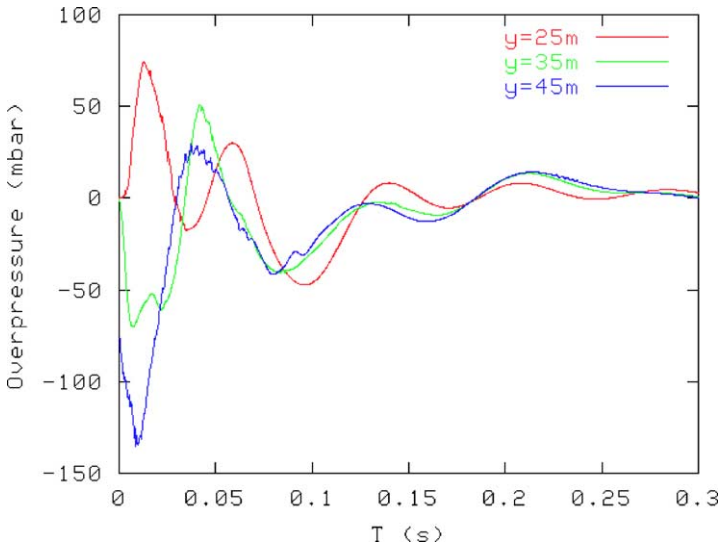

Fig. 19. Plot of overpressure with time for three different points along the street in front of the truck, at distances of approximately 3.5, 13 and 23 m from the ignition point ($y = 45$, 35 and 25 m, respectively, from the street corner), at positions close to the building wall closest to the truck and at a height of $z = 1.35$ m. These are results from the second step of the combustion simulation, beginning at $t = 90$ ms from the start of the first combustion simulation.

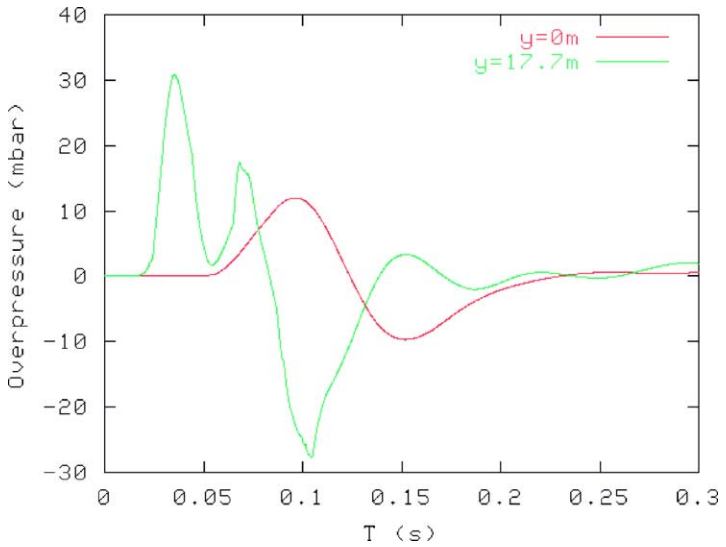

Fig. 20. Plot of overpressure with time for two different points along the street in front of the truck, at distances of 27 and 45 m from the ignition point ($y = 0$ and 17.7 m, respectively, from the street corner), at positions close to the building wall closest to the truck and at a height of $z = 1.35$ m. These are results from the second step of the combustion simulation, beginning at $t = 90$ ms from the start of the first combustion simulation.

discrepancy may be due to the fact that the grid used here is very coarse. This will cause a smearing out of the pressure wave and will cause an underprediction of the maximum overpressure.

6. Conclusions

In this paper the CFD approach has been successfully applied to the simulation of the 1983 Stockholm hydrogen accident. It has been demonstrated that CFD techniques are valuable tools for performing safety analysis for hydrogen systems. More specifically the following conclusions were drawn.

The complicated hydrogen release, consisting of a system of 18 interconnected steel pressure vessels (50 l each at 200 bar), was modelled in detail using a separate source model and using real hydrogen properties. It was found that, replacing the 18 bottles with one of equivalent volume, while keeping the same number of openings, results in only a 4% overprediction of the released hydrogen mass at 50 s after the start of release.

The dispersion calculations were used to identify the regions of the flow where ignition could have taken place. The ignition time was estimated to be 10 s after the start of release based on the accident report. At this time it was found that the flammable hydrogen mass and cloud volume reached their maximum values of 4.5 kg and 600 m^3, respectively. The predicted flammable cloud at 10 s was found to be restricted in the cross-street direction, extended along the street and with its height increasing with distance from the truck. This cloud behaviour was attributed to the strong horizontal momentum effects close to the source, the strong buoyancy effects away from it and the ambient atmospheric conditions. The dispersion calculations supplied the necessary initial conditions for both mean flow and turbulence for the subsequent combustion calculations.

Combustion calculations were performed based on the data supplied by the dispersion calculations. These calculations showed that a turbulent flame propagated through the flammable hydrogen cloud. The flame accelerated due to turbulence, mainly generated by obstacles. However, the flame did not reach the regimes of fast deflagration or detonation as indicated by the relatively limited overpressures generated by the flame (maximum overpressure of approximately 1000 mbar).

These results are to a large extent compatible with the reported accident consequences, both in terms of near-field damage to building walls and persons, and in terms of far-field damage to windows. Minor discrepancies are probably due to the very coarse mesh employed for the far-field simulation of the pressure wave caused by the explosion.

The present results demonstrate that hydrogen explosions in practically unconfined geometries will not necessarily result in fast deflagration or detonation events, even when the hydrogen concentration is in the range where such events could occur in more confined situations.

This work also underlines the importance of performing safety studies for hydrogen applications, in order to be able to understand, and therefore, minimise and control the consequences of accidental hydrogen releases to acceptable levels.

Acknowledgements

The authors would like to thank the European Commission for funding of this work in the framework of the EC project EIHP-2 (European Integrated Hydrogen Project).

References

[1] N.J. Duijm, B. Carissimo, A. Mercer, C. Bartholome, H. Giesbrecht, Development and test of an evaluation protocol for heavy gas dispersion models, J. Hazard. Mater. 56 (1997) 273–285.
[2] J. Würtz, J.G. Bartzis, A.G. Venetsanos, S. Andronopoulos, J. Statharas, R. Nijsing, A dense vapour dispersion code package for applications in the chemical and process industry, J. Hazard. Mater. 46 (1996) 273–284.
[3] B.H. Hjertager, T. Solberg, A review of computational fluid dynamics (CFD) modelling of gas explosions, in: V.E. Zarko, et al. (Eds.), Prevention of Hazardous Fires and Explosions, Kluwer Academic Publishers, Dordrecht, 1999, pp. 77–91.
[4] F.P. Lees, Loss Prevention in the Process Industries, vol. 2, Butterworths, UK, 1980.
[5] A.C. Vandenberg, A. Lannoy, Methods for vapour cloud explosion blast modelling, J. Hazard. Mater. 34 (2) (1993) 151–171.
[6] H. Wilkening, A.G. Venetsanos, T. Huld, J.G. Bartzis, Safety assessment of hydrogen as a fuel for vehicles by numerical simulation, in: Proceedings of the Euro-Conference on New and Renewable Technologies for Sustainable Development, Madeira Island, Portugal, June 26–29, 2000.
[7] J.G. Bartzis, ADREA-HF: a three-dimensional finite volume code for vapour cloud dispersion in complex terrain, Report EUR 13580 EN, 1991.
[8] H. Wilkening, T. Huld, An adaptive 3D CFD solver for modelling explosions on large industrial environmental scales, Combust. Sci. Technol. 149 (1999) 361–388.
[9] W. Breitung, G. Necker, B. Kaup, A. Veser, Numerical simulation of hydrogen in a private garage, in: Proceedings of the Fourth International Symposium on Hydrogen Power—Theoretical and Engineering Solutions—Hypothesis IV, Stralsund, Germany, September 9–14, 2001.
[10] Gasexplosionen på Brahegatan I Stockholm den 3 Mars 1983, Kommittén (Kn 1981:02) för undersökning av allvarliga olyckshäandelser, Utredningsrapport Nr.2, 1983, Stockholm (summarized translation in English).
[11] Encyclopedie des gaz, L'Air Liquide, Division Scientifique, Elsevier, Amsterdam, 1976, VII.
[12] J.E.A. John, Gas Dynamics, Alyn and Bacon, Inc., 1978.
[13] G. Rogers, Y. Mayhew, Engineering Thermodynamics Work and Heat Transfer, 4th ed., Longman, Copyright 1992.
[14] F. Grasso, C. Meola, Euler and Navier–Stokes equations for compressible flows: finite volume methods, in: R. Peyret (Ed.), Handbook of Computational Fluid Mechanics, Academic Press, London, 1996.
[15] S. Andronopoulos, J.G. Bartzis, J. Würtz, D. Asimakopoulos, Modeling the effects of obstacles on the dispersion of denser than air gases, J. Hazard. Mater. 37 (1994) 327–352.
[16] B.H. Hjertager, Computer modelling of turbulent gas explosions in complex 2D and 3D geometries, J. Hazard. Mater. 34 (1993) 173–197.
[17] G.W. Koroll, R.K. Kumar, E.M. Bowles, Burning velocities of hydrogen–air mixtures, Combust. Flame 94 (1993) 330–340.
[18] B.H. Hjertager, Simulation of gas explosions, Model. Ident. Contr. 10 (1989) 227–247.
[19] A.G. Venetsanos, N. Catsaros, J. Würtz, J.G. Bartzis, The DELTA_B code. A computer code for the simulation of the geometry of three-dimensional buildings. Code structure and users manual, EUR Report 16326 EN, 1995.